ACS OMEGA

http://pubs.acs.org/journal/acsodf

Article

Kumagawa and Soxhlet Solvent Fractionation of Lignin: The Impact on the Chemical Structure

Rosarita D'Orsi, Jeannette J. Lucejko, Francesco Babudri, and Alessandra Operamolla*

Cite This: *ACS Omega* 2022, 7, 25253−25264

Read Online

ACCESS | Metrics & More | Article Recommendations | Supporting Information

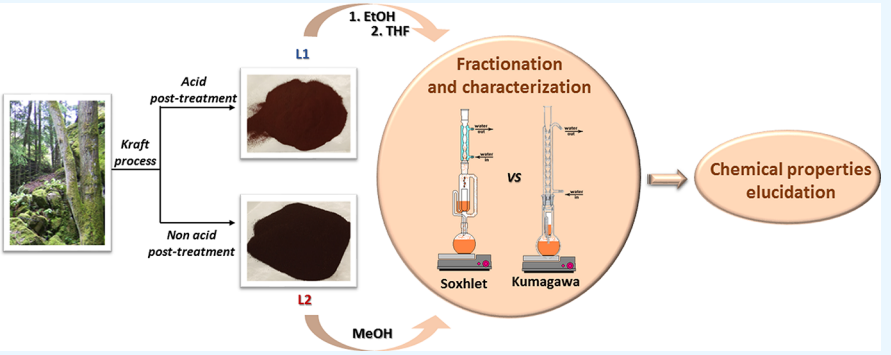

ABSTRACT: We investigated the effects of solvent fractionation on the chemical structures of two commercial technical lignins. We compared the effect of Soxhlet and Kumagawa extraction. The aim of this work was to compare the impact of the methods and of the solvents on lignin characteristics. Our investigation confirmed the potentialities of fractionation techniques in refining lignin properties and narrowing the molecular weight distribution. Furthermore, our study revealed that the Kumagawa process enhances the capacity of oxygenated solvents (ethanol and tetrahydrofuran) to extract lignin that contains oxidized groups and is characterized by higher average molecular weights. Furthermore, the use of tetrahydrofuran after ethanol treatment enabled the isolation of lignin with a higher ratio between carbonyl and other oxidized groups. This result was confirmed by attenuated total reflectance-Fourier transform infrared spectroscopy (ATR-FTIR), ^{13}C NMR and two-dimensional (2D) NMR spectroscopies, gel permeation chromatography (GPC), and analytical pyrolysis-gas chromatography−mass spectrometry (Py-GC−MS) analysis. Ultraviolet−visible (UV−vis) spectra evidenced the enrichment in the most conjugated species observed in the extracted fractions. Elemental analyses pointed at the cleavage of C-heteroatom bonds enhanced by the Kumagawa extraction.

INTRODUCTION

Lignin represents an abundant feedstock with potential attractive applications[1] but its use is limited because of its very complex and heterogeneous structure. So far, most of the lignin produced worldwide is burnt only for energy recovery.[2] Researchers are making several efforts to develop polymeric materials from lignin and use them as an alternative to petrochemicals.[3,4] However, lignin molecular weight distribution, functional group content, and heterogeneity of the structure depend on the different biomass feedstocks and on the method of extraction.[5,6] Therefore, the availability of lignin with well-defined mass ranges or with sufficient structural information appears difficult but, at the same time, it is a key requirement for the exploitation of this valuable resource. With this respect, fractionation procedures performed on lignin feedstocks can be an excellent approach to selecting and refining lignin characteristics.[7−12] The most used industrial lignin separation processes are kraft, sulfite, and soda pulping. Soda pulping can provide sulfur-free lignin, while the kraft process furnishes lignin containing sulfur in the form of thiol groups.[13,14] The sulfite process provides lignin with the highest sulfur content, as sulfonate moieties.[15] Nowadays, sulfur-free lignin is potentially more suitable for polymeric applications due to environmental policies. Within this framework, in this work, we selected two commercially available and sulfur-containing technical lignins, labeled **L1** and **L2**. Both lignins were derived from softwood by the kraft process, with the difference that the post-treatment was acid in the case of **L1** and alkaline in the case of **L2**. Furthermore, **L2** was judged by the provider to display a lower sulfonate content, as these groups would be produced by the acid treatment facilitating the oxidation of SH groups to sulfonic acids. To these technical lignins, we applied two different fractionation

Received: April 7, 2022
Accepted: June 3, 2022
Published: July 11, 2022

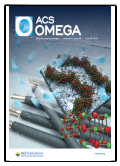

https://doi.org/10.1021/acsomega.2c02170
ACS Omega 2022, 7, 25253−25264

methods, based on continuous hot solvent extraction, performed using either a Soxhlet or a Kumagawa extractor. In a Kumagawa extractor, the thimble holder and the siphon are suspended above the boiling solvent, being maintained by the solvent vapor at a higher temperature than in an apparatus with a Soxhlet design. This determines the capacity to extract substances with higher melting points and enables specific applications, for instance, in bitumen extraction.[16] To the best of our knowledge, the Kumagawa extractor was never applied to lignin fractionation. Given the quite different solubility in organic solvents displayed by **L1** and **L2**, ethanol and tetrahydrofuran (THF) were used in sequence to fractionate **L1** lignin, while methanol was used to fractionate **L2** lignin. After performing the separation by the Kumagawa or Soxhlet apparatuses, the isolated fractions were characterized by attenuated total reflectance-Fourier transform infrared spectroscopy (ATR-FTIR), ultraviolet−visible (UV−vis) spectroscopy, ^{13}C NMR and two-dimensional (2D) NMR spectroscopies, elemental analyses, gel permeation chromatography (GPC), and analytical pyrolysis (Py-GC-MS). Comparing the analyses performed on the fractions with the properties of the corresponding original feedstocks, we not only obtained some information on the lignin structure but also evaluated the impact of the fractionation methods and the role of the solvents in the molecular structures.

EXPERIMENTAL SECTION

Materials. The lignin used in this study was purchased from Sigma-Aldrich. The **L1** lignin is the product no. 370959, while **L2** is the product no. 471003. The two lignins were used as received. Analytical grade solvents such as absolute ethanol (EtOH), tetrahydrofuran (THF), methanol (MeOH), ethyl acetate (EtOAc), cyclohexane, and dimethyl sulfoxide (DMSO) were purchased from Sigma-Aldrich. DMSO-d_6 for NMR spectra with 99.9 atom % D enrichment was obtained from Acros Organics.

pH Measurement. The pH values were measured at 24 °C using a pH meter Hanna instrument (product HI5521) equipped with a glass-body combination pH electrode (product HI1131B) and a temperature probe (HI7662-W). A 5% aqueous suspension of **L1** was prepared using 2 g of **L1** in 40 g of distilled water. **L1** did not dissolve in water and the measurement was performed in a heterogeneous system. This suspension gave a pH value of 6.84. A 3% aqueous solution of **L2** was prepared using 1 g of **L2** in 33.3 g of distilled water. The pH value of the clear solution obtained was 9.96.

Fractionation of Lignin. Two fractionation methods were performed using a 70 mL Kumagawa or Soxhlet apparatus. Each experiment was run in duplicate on a 3 g scale of starting material. **L1** lignin was first extracted with ethanol and subsequently, tetrahydrofuran was used as the second extraction solvent. **L2** lignin was extracted only with methanol. The temperature was increased to 20 °C above the solvent boiling temperature to obtain a constant reflux of liquid in the extraction chamber. The extraction process was allowed to proceed for 8 h. After extraction completion, the insoluble fraction was collected, while the solubilized lignin was recovered by evaporation under reduced pressure. Each fraction was dried *in vacuo* at a temperature of 55 °C until constant weight was reached.

Acetylation Procedure. The acetylation procedure used was based on the modified Manson's method.[17] The reaction was performed with a 2:1 weight ratio of acetic anhydride to lignin and 1-methylimidazole as a catalyst (0.05 mL/g of lignin) at 55 °C under a nitrogen atmosphere and vigorous stirring overnight. The mixture was quenched with ethyl acetate and washed five times with brine. Acetylated lignin samples were recovered by precipitation with cyclohexane, filtration, and drying *in vacuo* for 8 h. ATR-FTIR analysis was used to check the success of the acetylation reaction.[18]

ATR-FTIR Analysis. ATR-FTIR spectra were collected using a Thermo Fischer Nicolet iS50 FTIR instrument interfaced with an ATR ITX accessory equipped with a diamond crystal (radiation penetration approximately 2 μm at 1000 cm^{-1}). The spectra were recorded at room temperature in air in the range between 4000 and 650 cm^{-1} with a resolution of 4 cm^{-1}, 16 accumulated scans, and deuterated triglycine sulfate (DTGS) as a detector. The spectra were elaborated using OMNIC software.

UV−vis Absorption Spectroscopy. UV−vis absorption measurements were performed on 0.5 mg/mL solutions of lignin in DMSO at room temperature using a JASCO V-750 spectrophotometer and 0.1 cm path quartz cuvettes.

^{13}C NMR Sample Preparation and Analysis. Hydroxyl determination by ^{13}C NMR was performed on acetylated lignin samples. To perform ^{13}C NMR experiments, 150 mg of samples was dissolved in 1 mL of DMSO-d_6. The solutions were clear and no insoluble fractions were detected.

Experiments were carried out on a JEOL YH spectrometer with a probe operating at 100 or 125 MHz and conducted at 50 °C. Chemical shifts were given relative to tetramethylsilane and the position of peaks was referenced to the residual solvent peak of DMSO-d_6 (δ = 39.5 ppm). The spectra were quantitative and acquired with a 23 kHz (228 ppm) spectral width, 32 000 data points, an 11 s relaxation delay for a 75° pulse, zero-filling, and 10 Hz line broadening. The spectra were analyzed using JEOL Delta software.

2D NMR. To perform heteronuclear single quantum coherence (HSQC) experiments, 80 mg of samples was dissolved in 0.7 mL of DMSO-d_6. The analysis was carried out on a JEOL YH spectrometer with a probe operating at 400 MHz with spectral widths from 10 to 0 ppm and from 170 to 0 ppm for the ^{1}H- and ^{13}C- dimensions, respectively. The number of collected complex points was 2048 for the ^{1}H-dimension with a recycle delay of 1.5 s. The number of transients was 32, and 256 time increments were always recorded in the ^{13}C-dimension. Prior to Fourier transformation, the data matrices were zero-filled up to 1024 points in the ^{13}C-dimension. The central solvent peak was used as an internal reference (δ_C 39.5; δ_H 2.49).

Ash Content. The ash content was determined with a muffle furnace at 525 °C over 5 h. For **L2** lignin and its Soxhlet and Kumagawa residues, **L2-Sres** and **L2-Kres**, the furnace was kept at 600 °C for 7 h and the procedure was repeated until a constant mass of ash was achieved (after four cycles). All of the determinations were done in duplicate.

Elemental Analyses. Elemental analyses were performed on an Elementar Vario Micro Cube analyzer. Carbon, hydrogen, nitrogen, and sulfur contents were determined for the commercial **L1** and **L2** lignin for the respective acetylated samples (Table S1) and for all fractions collected after the fractionation processes. All analyses were carried out on 5 mg samples to evidence well changes in the sulfur or nitrogen content. The oxygen content was calculated for all samples by the difference after ash correction. Instead, **L1** and **L2** were determined directly. All determinations were done in duplicate.

https://doi.org/10.1021/acsomega.2c02170
ACS Omega 2022, 7, 25253−25264

GPC Analysis. Gel permeation chromatography (GPC) analysis was carried out at room temperature using a Malvern Viscotek TDA 305 equipped with a Tosoh Bioscience TSK gel G3000HHR column (7.8 mm i.d. x 30.0 cm l) using a refractive-index detector with chloroform as solvent. Calibration was performed using polystyrene standards. The acylated lignin samples were dissolved in chloroform at a 1 mg mL^{-1} concentration and filtered prior to the measurement with 0.22 mm PTFE filters.

Analytical Pyrolysis. Thepyrolysis-gas chromatography/mass spectrometry (Py-GC/MS) experiment was performed with an EGA/PY-3030D microfurnace pyrolyzer (Frontier Laboratories, Japan) coupled to an 8890 gas chromatograph and a 5977 mass spectrometric detector (Agilent Technologies). Approximately, 100−200 μg of the sample was used. Pyrolysis was performed at 550 °C with an interface temperature of 280 °C. The injection was performed in a split mode with a 1:5 ratio at 280 °C. The separation of the pyrolysis products was achieved with an HP-5MS fused silica capillary column (30 m × 0.25 mm, film thickness 0.25 μm, Agilent Technologies) and helium (1 mL min^{-1}) as a carrier gas. The temperature program of the GC oven was 40 °C isothermal for 5 min, 15 °C min^{-1} up to 280 °C, and 280 °C isothermal for 20 min. The mass spectrometer was operated in an EI positive mode (70 eV, m/z range 40−500). The transfer line temperature was 280 °C.

The identification of lignin pyrolysis products, listed in Table S1, was based on literature data[19,20] and NIST library 2.4. Semiquantitative calculations were performed on chromatographic areas of lignin pyrolysis products recognized and integrated by Automated Mass spectral Deconvolution and Identification System (AMDIS) software.[21] Peak areas were normalized with respect to the sum of the peak areas of all lignin pyrolysis products identified, and the data were averaged and expressed as percentages. The percentage areas were used to calculate the relative abundances of lignin pyrolysis products divided into categories based on their chemical structure and listed in Table S1. Six categories were selected for lignin pyrolysis products: "short side chain" aromatic compounds (*p*-hydroxyphenyl and guaiacyl units with up to a C2 alkyl substituent on the aromatic ring), "long side chain" compounds (*p*-hydroxyphenyl and guaiacyl units with a C3 alkyl substituent on the aromatic ring), "monomers" (coniferyl alcohols, which show an unaltered side chain), "carbonyl compounds" (*p*-hydroxyphenyl and guaiacyl units containing aldehyde and ketone functionalities), "demethylated" compounds (guaiacyl units in which one methyl group was removed from the methoxy substituent), and "dimers" (lignin-derived diphenolic products).

RESULTS AND DISCUSSION

Lignin Fractionation. The two fractionation procedures were carried out with the use of either a Kumagawa or a Soxhlet extractor. The selection of a suitable solvent for the extraction was based on the room temperature solubility displayed by each lignin. Therefore, **L1** lignin was fractionated in sequence with ethanol and tetrahydrofuran, while **L2** lignin, insoluble in THF, was extracted with methanol, which was a more efficient oxygenated solvent for this lignin compared to ethanol. The extraction yields and the names of the fractions are summarized in Table 1. For easy reference, the fractions are named with the acronyms **L1-X** and **L2-X**, distinguishing the parent lignin **L1** or **L2**, with **X** being a letter indicating the extraction method, namely **S** for Soxhlet and **K** for Kumagawa. The numbers are referred to the first or second solvent and "res" is referred to the recovered insoluble fraction. The extraction yields were maximized by the Kumagawa process due to the higher temperature of the thimble in the extraction apparatus. This effect was particularly noticeable in the fractionation of **L1**, whose insoluble residue left by the Kumagawa treatment was only 25% compared to 67% residue left by the Soxhlet fractionation with the same solvents.

Table 1. Fraction Names and Extraction Yields for L1 and L2 Lignin

starting lignin	extraction solvent	Kumagawa[a]	Soxhlet[a]
L1	EtOH[b]	**L1-K1** (13%)	**L1-S1** (3%)
	THF[c]	**L1-K2** (62%)	**L1-S2** (30%)
		L1-Kres (25%)	**L1-Sres** (67%)
L2	MeOH[d]	**L2-K1** (40%)	**L2-S1** (30%)
		L2-Kres (60%)	**L2-Sres** (70%)

[a]Fraction name and yield in parentheses are reported in this column. [b]Used as the first solvent of extraction. [c]Used as the second solvent of extraction after ethanol. [d]Used as the sole solvent of extraction.

ATR-FTIR Spectroscopy. ATR-FTIR spectroscopy was employed to analyze the chemical characteristics of each lignin fraction recovered after solvent extraction. FTIR spectra, indeed, can furnish useful information about the presence of functional groups and the efficiency of the selected solvent in extracting the most oxidized fractions.[22] The spectra of the parent materials, **L1** and **L2** lignin, are reported in Figure 1.

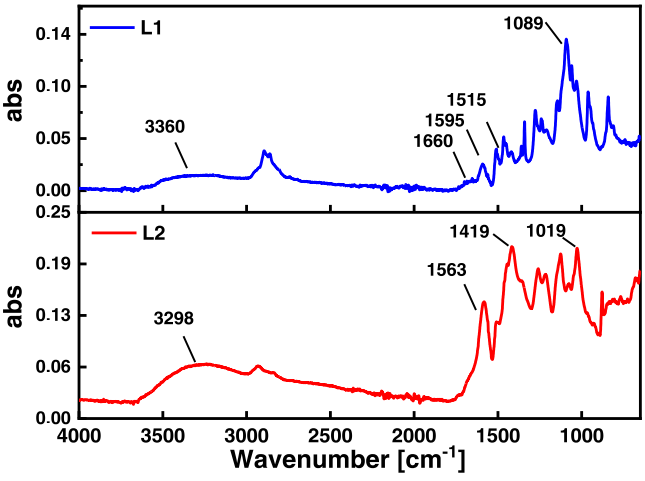

Figure 1. ATR-FTIR spectra of **L1** (top panel) and **L2** (bottom panel) lignin.

Characteristic peaks are evident in the 3800−2700 and 1850−700 cm^{-1} spectral regions.[23,24] Both lignins present a broad absorption band that can be attributed to the stretching vibration of phenolic and aliphatic O−H groups. This band in **L1** is centered at 3360 cm^{-1} and in **L2** lignin at 3298 cm^{-1}. Furthermore, aromatic and aliphatic C−H stretching can be related to signals in the 3050−2800 cm^{-1} spectral range. The two lignin profiles appear quite different between 1000 and 1500 cm^{-1}, indicating differences in the C−O stretching modes of ethers and alcohols. The pronounced peak at 1089 cm^{-1} in **L1** lignin suggests the presence of a higher concentration of aliphatic ethers than in **L2** lignin. In the **L2** profile, the pronounced peaks at 1419 and at 1019 cm^{-1}

https://doi.org/10.1021/acsomega.2c02170
ACS Omega 2022, 7, 25253−25264

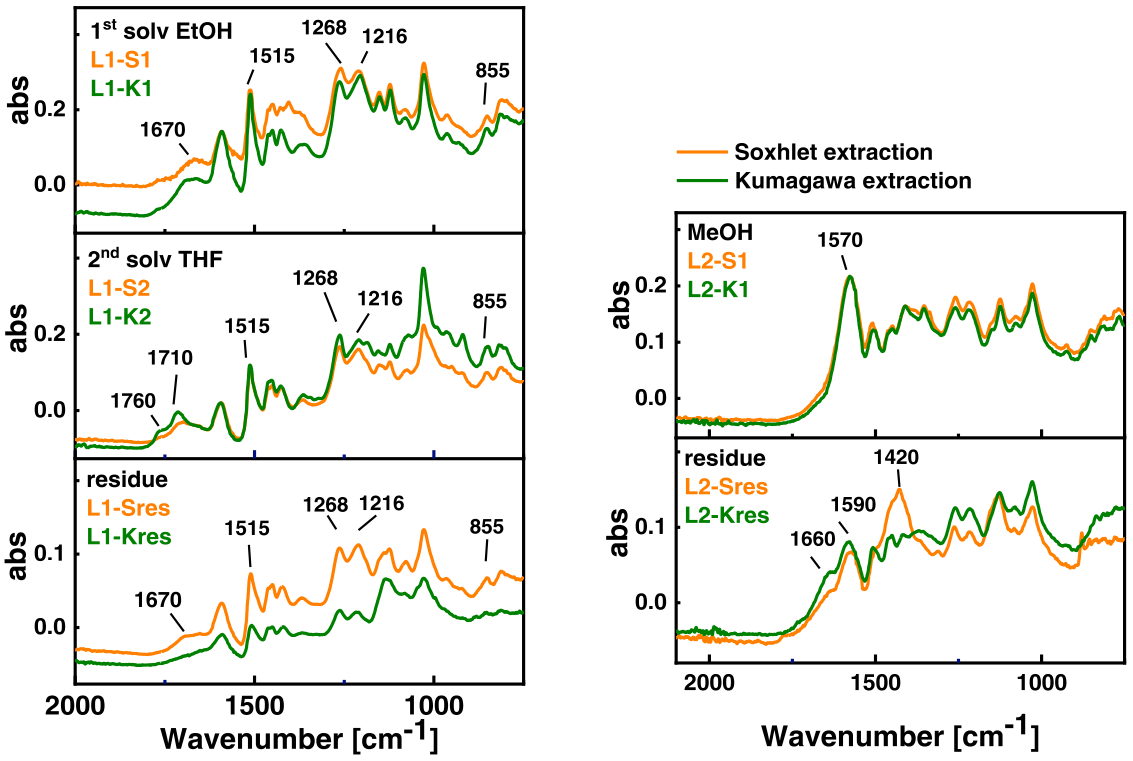

Figure 2. ATR-FTIR spectra of **L1** (a, left panel) and **L2** (b, right panel) Soxhlet and Kumagawa extracted fractions. The spectra of the fractions derived from the Soxhlet process are represented in orange. The spectra of the fractions derived from the Kumagawa process are presented in green.

suggest the presence of phenolic OH groups and aromatic ethers, respectively. In the **L1** profile, aromatic signals in the range of 1500−1515 cm^{-1} are more evident, while the peaks in the range of 1600−1700 cm^{-1} suggest the presence of more carbonyl moieties than in **L2** lignin.

The ATR-FTIR spectra recorded after fractionation are reported in Figure 2, with enlarged views in the 1850−700 cm^{-1} region, where the diagnostic peaks of lignin are present. The spectra of the fractions derived from Soxhlet extraction are presented in orange color, while the spectra of the fractions deriving from Kumagawa extraction are shown in green. All spectra are characterized by the presence of a peak at ∼1500 cm^{-1} that is typical of aromatic skeletal vibrations in lignin.[25] All fractions present two peaks at 1268 and 1216 cm^{-1} that are attributed to the stretching of guaiacyl moieties, confirmed by the presence of distinguishable peaks at 855 and 817 cm^{-1}, assigned to the C−H out-of-plane deformation in G units. The signals between 1660 and 1710 cm^{-1} show the presence of oxidized species in all extracted fractions and residues of **L1**. These signals are attributable to the stretching vibration of the C═O bonds in conjugated aldehydes and carboxylic acids.[26] These species are present in ethanol and THF fractions (peak position at 1670 cm^{-1}). In THF fractions, the absorption in the range 1710−1760 cm^{-1}, related to unconjugated ketones and esters, appears much more significant than in the ethanol fractions. The favorable ratio between carbonyl absorption/other oxidized species' absorption appears much more pronounced in the THF Kumagawa fraction, **L1-K2**. **L1-Kres** shows the lowest concentration in oxidized species, which was concentrated in the soluble fractions by the Kumagawa process. Conversely, the extraction residue derived from Soxhlet treatment, **L1-Sres**, displays a nearly unchanged content of species with carbonyl and carboxyl functionalities with respect to the parent lignin. These differences point clearly at an enhanced capacity of the Kumagawa process to extract especially carbonyl and other oxidized fractions of lignin when using polar solvents. In our view, this signifies that the Kumagawa fractionation using ethanol and THF in sequence may be a valuable way to concentrate carbonyl groups with respect to other oxidized moieties of technical lignins in THF fractions. This enrichment apparently results from the polar interactions (either hydrogen bonding or dipole) between the extracting solvent and lignin.[22,24] THF displays an enhanced attitude to yield a higher extraction yield (60%) and selectivity toward carbonyl compounds over other oxidized species.

While **L1** fractions yielded ATR-FTIR spectra evidencing complex differences in the molecular structure, no relevant differences were found in lignin **L2** Kumagawa or Soxhlet fractions FTIR profiles: both methods left oxidized enriched species in the residue. The Soxhlet process left phenolic alcohols mostly in the residue, as evidenced by a pronounced peak at 1420 cm^{-1}. Switching from Soxhlet to Kumagawa extraction generated only an increase in the extraction yield (40% of isolated **L2-K1** vs 30% of isolated **L2-S1**).

UV−vis Absorption Spectra. Lignin absorption in the UV−vis region is related to its aromatic structure, conjugated with aliphatic double bonds and carbonyls.[27] We carried out UV−vis measurements dissolving each lignin fraction in dimethyl sulfoxide, which allowed for their complete solubilization. The absorption spectral range is limited for this reason to wavelengths longer than 260 nm. In the normalized spectra (Figure 3), all fractions displayed a maximum absorption peak at around 286 nm that can be

https://doi.org/10.1021/acsomega.2c02170
ACS Omega 2022, 7, 25253−25264

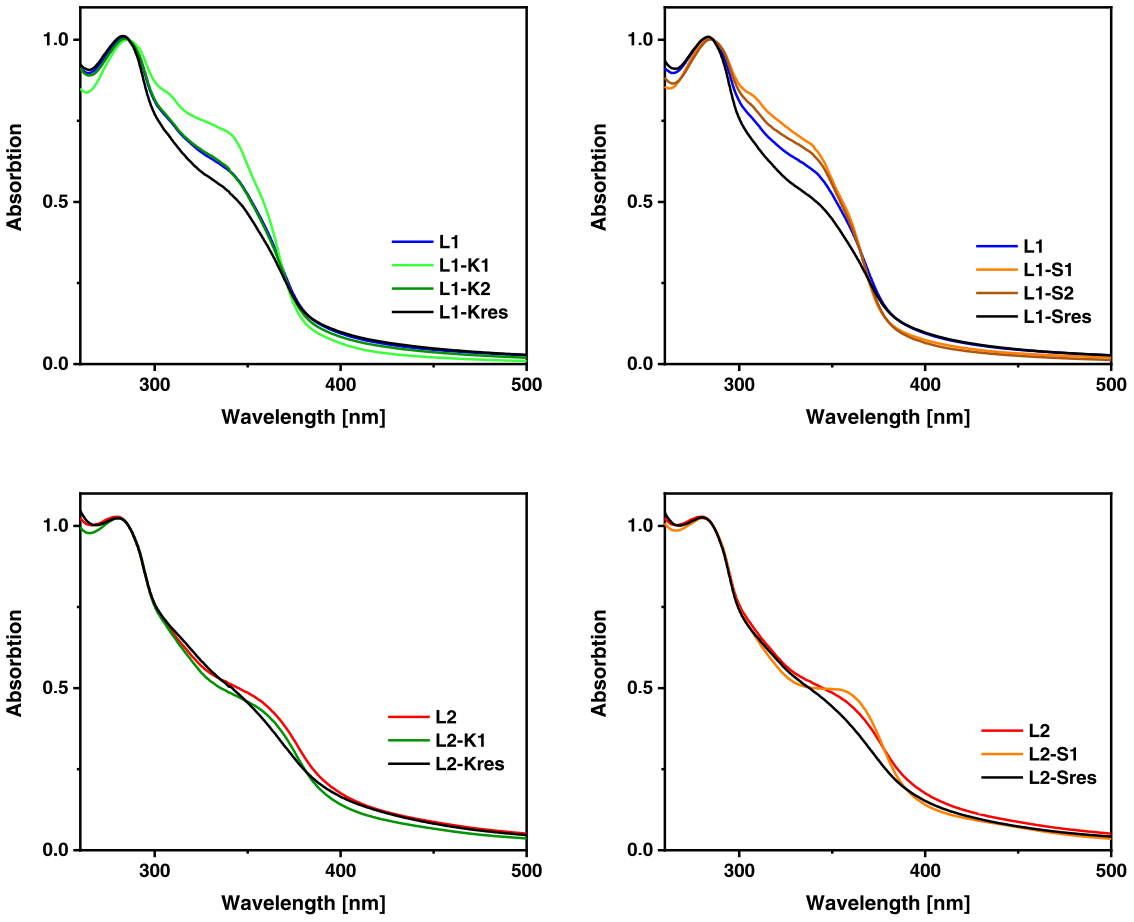

Figure 3. Normalized UV−vis spectra of extraction fractions compared with parent lignin.

referred to as noncondensed phenolic groups in guaiacyl units, whose presence was also confirmed by ATR-FTIR spectra.[28] However, the two untreated lignins present different absorption profiles at the longest wavelength region: while **L1** lignin presents a peak at 341 nm that can be ascribed to α-carbonyl groups and esters of hydrocinnamic acid,[29] for **L2**, a peak of conjugated species can be found at 360 nm. The presence of such low-energy peaks in technical lignin samples could be ascribed to other conjugated structures such as stilbenes[30] or enol ethers.[31] These structures could appear due to the effect of depolymerization of the original polymer caused by a harsher treatment. In the ethanol (**L1-K1** and **L1-S1**) and methanol (**L2-K1** and **L2-S1**) extraction fractions, conjugated species are dissolved to a greater extent due to the enhanced absorption shoulder at higher wavelengths. This points to the presence of hydrogen bonding groups in the lignin fractions containing delocalized functionalities due to the higher affinity toward the alcoholic solvent. Conversely, the spectra of insoluble fractions (**L1-Kres**, **L1-Sres**, **L2-Kres**, **L2-Sres**, shown in black) present less pronounced peaks at these wavelengths, indicating a lower concentration of conjugated chromophores left in the extraction thimble at the end of the fractionation process.

Gel Permeation Chromatography. The effect of solvent fractionation was also observed on the average molecular weights and their distribution. We performed GPC analysis on the acetylated lignin samples to allow their complete dissolution in $CHCl_3$ for consistent comparison. Since lignin is far from being a coiled polymer, the differences between the polystyrene standards and the lignin macromolecules may be a large source of error.[7] Therefore, this analysis provides only a relative molecular weight quantification with respect to the standard used for calibration (*i.e.*, monodisperse polystyrene standards). Values of number-average molecular weight (M_n), weight-average molecular weight (M_w), and polydispersity index (PI) are reported in Table 2.

First of all, GPC measurements confirmed the more depolymerized structure of **L2**, corroborating what was

Table 2. Number- and Weight-Average Molecular Weights and Polydispersity Indices Resulting from GPC Analyses of Acetylated Lignin Samples and All Acetylated Fractions[a]

	M_n (Da)	M_w (Da)	PI
Ac-L1	2150	4830	2.3
Ac-L1-S1	1600	2260	1.4
Ac-L1-S2	2180	2800	1.3
Ac-L1-Sres	5840	10 700	1.8
Ac-L1-K1	1580	2080	1.3
Ac-L1-K2	2850	4900	1.7
Ac-L1-Kres	4070	6550	1.6
Ac-L2	1260	3390	2.7
Ac-L2-S1	1110	1420	1.3
Ac-L2-Sres	1010	1640	1.6
Ac-L2-K1	740	1020	1.4
Ac-L2-Kres	1580	2630	1.7

[a]Values were detected relative to polystyrene standards.

https://doi.org/10.1021/acsomega.2c02170
ACS Omega 2022, 7, 25253−25264

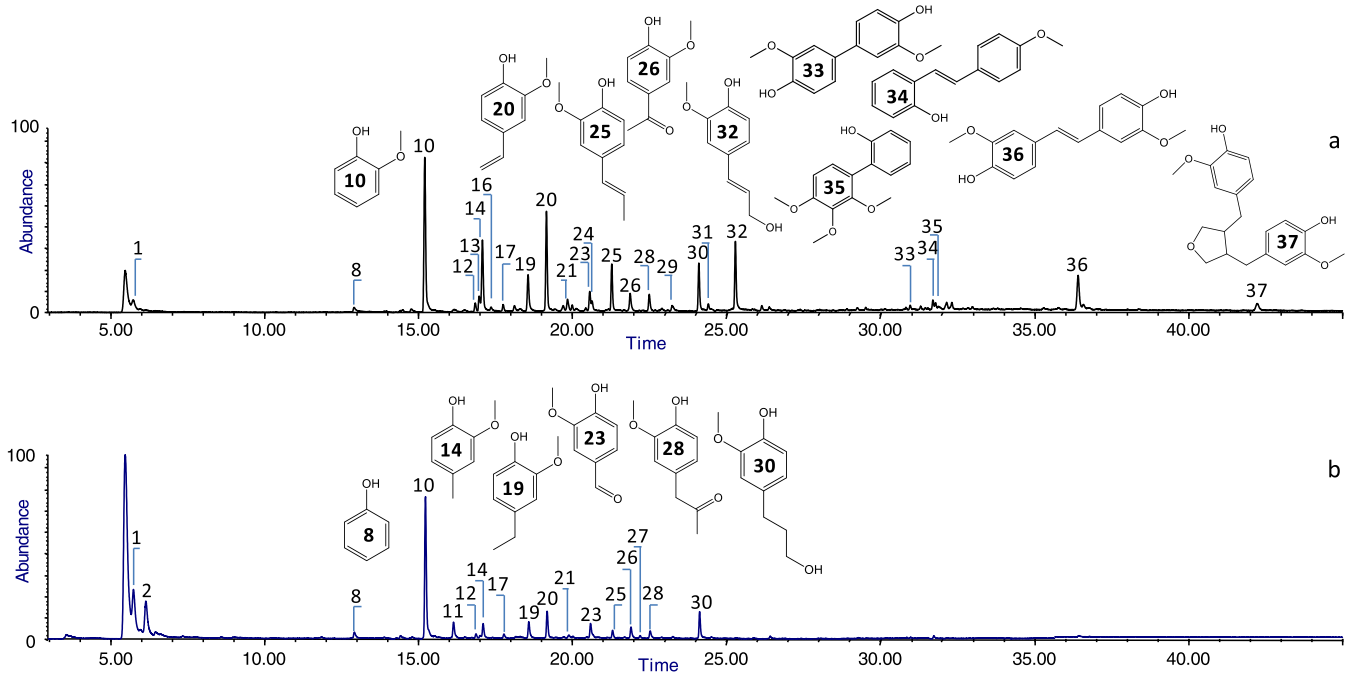

Figure 4. Chromatographic profiles obtained by Py-GC/MS for **L1** (panel a, top) and **L2** (panel b, bottom). Numbers refer to pyrolysis products listed in Table S1, (*)—carbon dioxide.

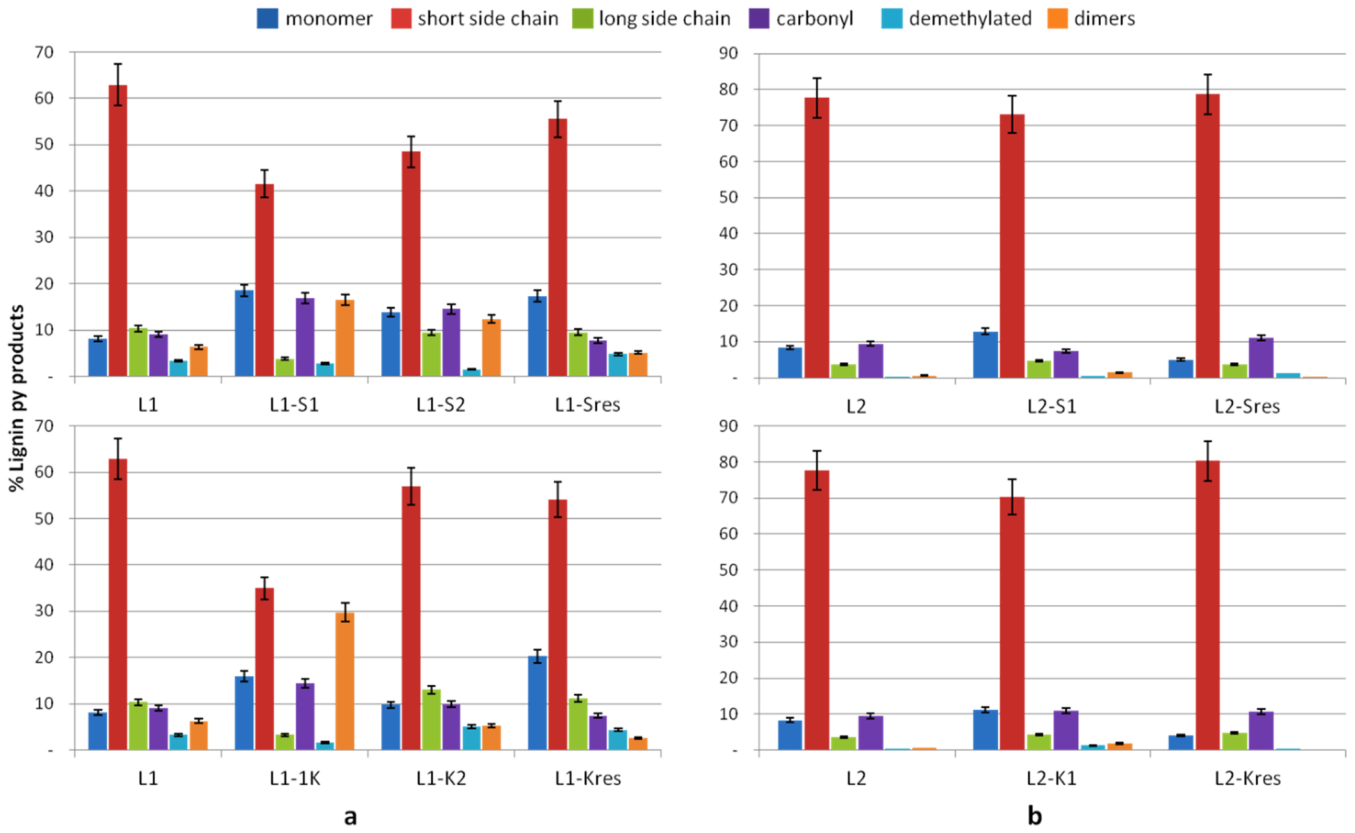

Figure 5. Distribution of lignin pyrolysis products obtained by Py-GC/MS from **L1** (panel a, left) and **L2** (panel b, right) and **L1-X** and **L2-X** fractions. Pyrolysis products were identified and classified as reported in Table S1, and are identified by the following color code: the monomer in blue, the short side chain in brown, the long side chain in green, carbonyl in violet, demethylated in light blue, and the dimer in orange.

deduced from FTIR and UV−vis spectra. Indeed, lower M_n and M_w were recorded for **L2**. Furthermore, **L2** displayed a higher polydispersity index than **L1**. **L2**'s nonhomogeneity could be due to the degradation processes it underwent during its production. GPC data supported the observed trend on the effect of solvent fractionation on **L1** and **L2**. Sequential extraction of **L1** by the Kumagawa or Soxhlet process was selective for lower-MW species, while higher-MW species were

https://doi.org/10.1021/acsomega.2c02170
ACS Omega 2022, 7, 25253−25264

left in the solid residue. Overall, the Soxhlet soluble fractions presented a narrower molecular weight distribution compared to the parent lignin **L1**. In particular, the THF fraction (**Ac-L1-S2**) showed a further reduction of polydispersity than the ethanol fraction (**Ac-L1-S1**). Conversely, the insoluble fraction, **Ac-L1-Sres**, presented the highest polydispersity index (1.8). The Kumagawa process allowed the dissolution of lignin with broader molecular weight distribution and higher average molecular weights in the THF fraction. The two fractionation processes applied to **L2** yielded soluble fractions (**Ac-L2-S1** and **Ac-L2-K1**) in both cases with lower average molecular weights and a lower polydispersity. In the case of **L2**, the Kumagawa and Soxhlet fractionation appear to produce a rather similar trend in the fractions' molecular weights. The general trend indicates that soluble fractions are relatively homogeneous in terms of molecular size, while insoluble fractions present higher molecular weights and polydispersity. The Soxhlet process appears to be more generally effective in narrowing molecular weight distribution with each solvent but less effective in terms of the extraction yield.

Analytical Pyrolysis. To assess the correct assignment of ATR-FTIR signals and UV−vis absorption maxima, analytical pyrolysis coupled with gas chromatography and mass spectrometry was performed on the parent lignins and their fractions. Figure 4 reports chromatographic profiles obtained for **L1** and **L2**. To have chromatographic peaks with comparable abundances, the amount of **L2** lignin had to be at least double that of **L1**. Despite this measure, the chromatographic profiles obtained for **L1** and **L2** differed both qualitatively and quantitatively. In **L1**, 29 pyrolysis products derived from lignin were determined against 23 products in **L2**. These products are listed and numbered in Table S1. The most abundant peak from both lignins was guaiacol (#10). Compounds such as catechol (#13), *Z*- and *E*-coniferyl alcohols (#31 and #32), as well as dimers (#33, #35, and #37) were present in **L1** and not detected in **L2**. The other pyrolysis products (#14, #19, #23, #28, and #30) were much more abundant in the **L1** profile than the **L2** one. The total absence of a guaiacyl lignin monomer, (*E*)-coniferyl alcohol (#32), and the much lower presence of lignin dimers (stilbene-like compounds, #36) in the **L2** profile allowed us to confirm conclusions about the method used to prepare **L2**: evidently, the process producing **L2** was harsher and more degrading than the one producing **L1**. Therefore, lignin **L2** appears more depolymerized than **L1**.

The results obtained from the same analysis performed on the fractions of these two lignins are summarized in Figure 5, with reference to the concentration of fragments in each soluble fraction and residue. Lignin fragments' composition obtained for **L1** and **L2** confirms the hypothesis that **L2** is more depolymerized than **L1**. In fact, the most abundant group appears to be that of products with a short side chain, which, in the case of **L2**, reaches 78%, compared to the 62% relative abundance of **L1**.

The first ethanol extraction step was performed by the Kumagawa process on **L1** preconcentrated higher boiling compounds such as dimers due to the higher temperature reached by the Kumagawa apparatus. The Soxhlet extractor, on the other hand, allowed for a better preconcentration of all of the other products, apparently generating a fraction enriched in carbonyl moieties. However, the lower yield of the **L1-S1** fraction (3%) with respect to **L1-K1** (13%) reveals the lower capacity of the Soxhlet process to exhaustively extract all oxidized fractions from the parent lignin. In the Kumagawa procedure, THF extraction appeared better for less polar compounds ("short side chain", "long side chain") than the Soxhlet one. The residues remaining after both extraction procedures apparently had a rather similar composition, with the macroscopic difference that **L1-Kres** and **L1-Sres** were isolated with dramatically different yields (25 and 67%, respectively).

In **L2** fractionation, no important differences were observed between the two applied procedures, except for the slightly greater ability of the Kumagawa process to extract products with carbonyl functionalities (10%), with respect to Soxhlet extraction (7%). This result was less surprising, considering the smaller difference between the extraction yields delivered by the two processes.

^{13}C NMR Spectra. A change in the total amount of OH groups and unsubstituted positions (C_{Ar}−H) on the aromatic ring is important to evaluate the occurrence of depolymerization or condensation processes during lignin fractionation. For this purpose, acetylation was performed on each lignin sample not only to enable GPC analysis but to determine the hydroxyl group content. So far, several procedures are documented in the literature for the determination of lignin hydroxyl groups' content.[32,33] We used nuclear magnetic resonance (NMR) spectroscopy acquired on acetylated derivatives, as a reliable technique for the analysis of typologies and concentration of different carbon atoms based on their chemical neighborhood. ^{13}C NMR spectroscopy, in fact, provides a detailed and clear determination of aliphatic and phenolic hydroxyls as acetyl esters. In all acetylated compounds, the assigned hydroxyl band in FTIR-ATR spectra was negligible and a new band appeared at 1730 cm^{-1} that revealed the ester group presence and was taken as an indication of the success of the acetylation reaction. **L1** and the corresponding acetylated product FTIR-ATR spectra are shown as an example of this procedure result in Figure 6.

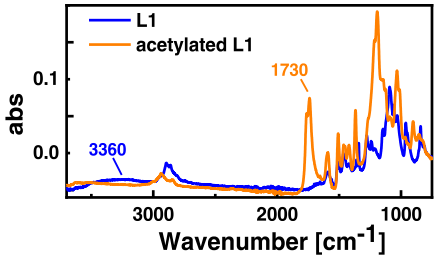

Figure 6. ATR-FTIR spectra of **L1** and its acetylation product.

The ^{13}C NMR spectrum of acetylated **L1** is reported in Figure 7. The inset shows an enlargement of the spectral region between 164 and 174 ppm, where the peaks corresponding to phenolic and aliphatic hydroxyl groups appear as acetyl esters. For the determination of the hydroxyl content, we used the following integration limits: from 171.2 to 169.9 ppm for primary aliphatic alcohols OH (I), from 169.9 to 169.4 ppm for secondary hydroxyls OH (II), and from 167.2 to 169.2 ppm for phenolic hydroxyls OH (Φ). These groups were detected as acyl (acetic ester) derivatives. The spectral range from 160 to 100 ppm includes aromatic carbons. We used the integration limits from 142 to 162 ppm to determine oxygenated aromatic carbons C_{Ar-O}, from 125 to 142 ppm to determine nonoxygenated aromatic carbons C_{Ar-C}, and from

https://doi.org/10.1021/acsomega.2c02170
ACS Omega 2022, 7, 25253−25264

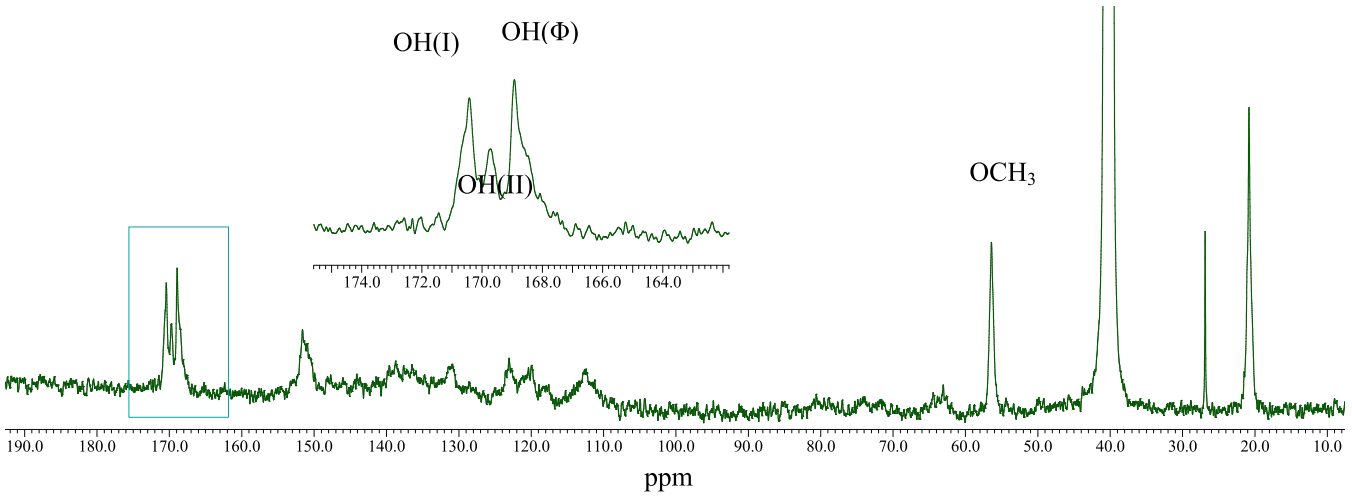

Figure 7. ^{13}C NMR of acetylated **L1** lignin. The inset shows an enlargement of the 164−174 ppm spectral region, where the acyl carbon of esters can be detected.

Table 3. Number of C Atoms and −OH Groups Per C_9 Unit Values Obtained from ^{13}C NMR of Acetylated Compounds

	OH(I)[a]	OH(II)[b]	OH(Φ)[c]	OH(tot)[d]	C_{Ar-O}[e]	C_{Ar-C}[f]	C_{Ar-H}[g]	aliphatic C−O[h]	OCH_3[i]
L1	0.35	0.15	0.49	0.99	0.56	0.75	1.04	0.93	0.59
L1-S1	0.26	0.16	0.59	1.01	0.53	0.44	0.43	0.01	0.71
L1-S2	0.27	0.18	0.55	1.00	0.65	0.89	1.20	0.33	0.69
L1-Sres	0.37	0.22	0.41	1.00	0.67	0.47	1.07	0.55	0.66
L1-K1	0.20	0.18	0.58	0.96	0.49	1.27	1.08	0.28	0.79
L1-K2	0.26	0.16	0.58	1.00	0.74	0.60	0.68	0.13	0.68
L1-Kres	0.33	0.23	0.44	1.00	0.62	0.33	0.69	0.15	0.78
L2	0.29	0.22	0.46	0.97	0.85	1.11	1.38	0.82	0.66
L2-S1	0.27	0.15	0.58	1.00	0.45	0.50	0.81	0.27	0.66
L2-Sres	0.33	0.22	0.46	1.01	0.69	0.77	1.13	0.33	0.74
L2-K1	0.31	0.18	0.51	1.00	0.49	0.15	0.46	0.14	0.80
L2-Kres	0.31	0.19	0.49	0.99	0.45	0.43	0.59	0.11	0.64

[a]Detected with integration limits: from 171.2 to 169.9 ppm for primary aliphatic hydroxyl groups. [b]From 169.9 to 169.4 ppm for secondary aliphatic hydroxyl groups. [c]From 169.2 to 167.2 ppm for the phenolic group. [d]From 167.2 to 171.2 for total hydroxyl groups. [e]From 142 to 162 ppm for oxygenated aromatic carbons C_{Ar-O}. [f]From 125 to 142 ppm for nonoxygenated aromatic carbons C_{Ar-C}. [g]From 100 to 125 ppm for protonated aromatic carbons C_{Ar-H}. [h]From 58 to 90 for aliphatic C−O. [i]From 54 to 58 ppm for the OCH_3 content.

100 to 125 ppm to determine protonated aromatic carbons C_{Ar-H}. The range from 58 to 90 ppm includes aliphatic carbons. In this region, we identified the $-OCH_3$ signal. Its content was determined by the integration of the signal between 54 and 58 ppm, corresponding to the OCH_3 groups in the guaiacyl units. Table 3 summarizes the values calculated by integration of the above-described individual contributions furnished by the ^{13}C NMR investigation for each lignin sample.

NMR analyses can reveal modification of the chemical structure of the treated lignin upon fractionation. A decrease in aliphatic, especially primary, and an increase in phenolic hydroxyl group content could be noticed in all of the solvent-extracted fractions with respect to the parent material for both **L1** and **L2** lignin. Conversely, the insoluble fractions, named **L1-Kres**, **L1-Sres**, **L2-Kres**, and **L2-Sres**, presented higher aliphatic −OH group content. This difference could be explained by the occurrence of depolymerization during the fractionation process, producing partial breaking of aryl−alkyl ether linkages. In the original **L2**, a higher content in oxygenated aromatic carbons C_{Ar-O} (0.85) with respect to phenolic hydroxyls −OH (0.46) points to the presence of a higher amount of aryl ether groups, which is maintained in the solid residue after extraction. The data agree with FTIR-ATR profiles. This ratio decreases in **L2-S1** and **L2-K1** fractions, confirming the capacity of hot solvent treatment to induce the partial rupture of aryl ether linkages.[19] In the Soxhlet THF fraction from **L1**, **L1-S2**, a significant increase in non-oxygenated aromatic carbon C_{Ar-H} is noticed (from 1.04 in **L1** to 1.20 in **L1-S2**). Since a decrease in the content of C_{Ar-H} suggests a higher degree of condensation due to the lack of free positions on the aromatic ring,[34] this observation indicates that the most linear lignin polymeric structures are extracted by THF in the Soxhlet process. This can be still true for the **L1-K1** ethanolic fraction, but the fraction **L1-K2**, extracted with THF by the Kumagawa apparatus, yields lignin with an apparently less linear structure, presenting a content of C_{Ar-H} of 0.68, very similar to 0.69, the value found for **L1-Kres**. Therefore, the decrease observed in all extracted fractions, including extraction residues, pointed at condensation processes, which may be activated by the fractionation procedure. Finally, none of the lignin showed detectable signals in the 100−90 ppm region, related to the carbohydrate presence, which therefore has to be below the NMR technique detection limit.

HSQC Experiments. Simple ^{1}H NMR of lignin would show overlapping resonances due to lignin interunit linkage

https://doi.org/10.1021/acsomega.2c02170
ACS Omega 2022, 7, 25253−25264

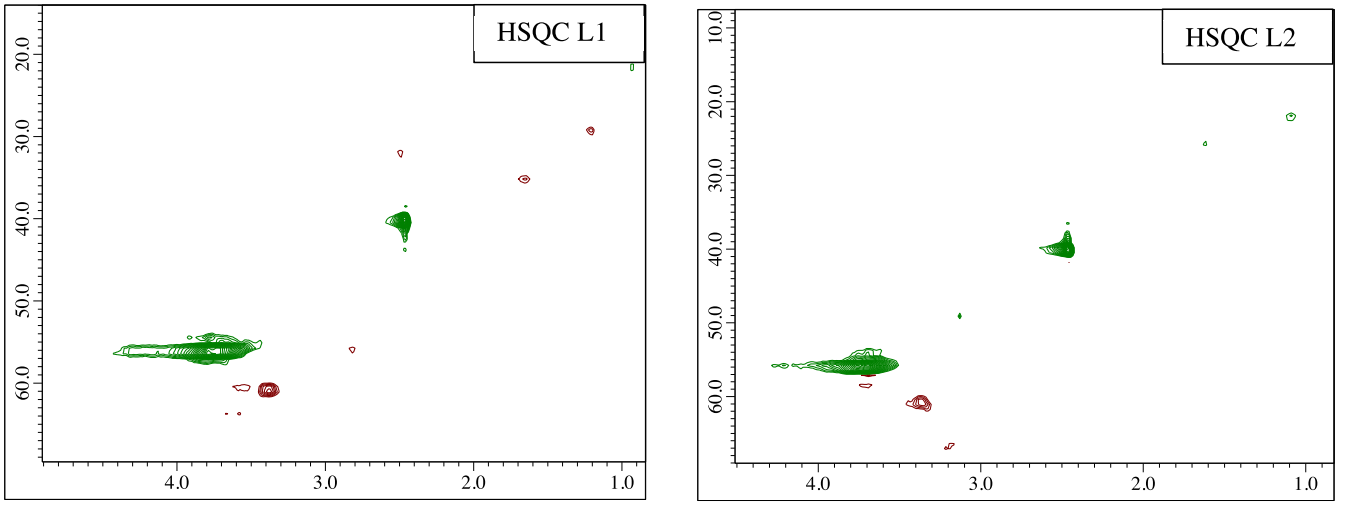

Figure 8. Enlargement in the aliphatic side chain of HSQC **L1** and **L2** spectra.

Table 4. Ash Content for L1, L2, and L2-Sres Fractions, Elemental Analysis Results, OCH_3 Unit Content in the Empirical Formula, Calculated Empirical Formula, and the Formula Weight of Each Lignin Sample

		elemental analysis (% w/w)							
lignin sample	ash (% w/w)	C	H	N	S	O	OCH_3[a]	empirical formula	F_w(g/mol)
L1	3.10	61.00	6.27	0.65	1.51	27.47[b,c]	1.16	$C_9H_{8.96}O_{2.27}S_{0.09}N_{0.09}(OCH_3)_{1.16}$	193.49
L2	25.32	46.57	5.19	0.07	1.68	21.17[b,c]	0.70	$C_9H_{10.77}O_{2.60}S_{0.12}N_{0.01}(OCH_3)_{0.70}$	186.16
L1-K1		62.78	6.70	0.35	0.80	29.37	1.46	$C_9H_{8.92}O_{2.22}S_{0.05}N_{0.05}$ $(OCH_3)_{1.46}$	200.12
L1-K2		62.70	6.46	0.21	0.90	29.73	1.44	$C_9H_{8.50}O_{2.28}S_{0.056}N_{0.03}(OCH_3)_{1.44}$	199.95
L1-Kres		60.21	6.37	0.43	2.09	30.90	1.02	$C_9H_{9.58}O_{2.84}S_{0.13}N_{0.06}(OCH_3)_{1.02}$	199.86
L1-S1		61.53	6.74	1.40	1.22	29.11	1.20	$C_9H_{9.78}O_{2.44}S_{0.08}N_{0.20}(OCH_3)_{1.20}$	199.50
L1-S2		63.30	6.71	0.12	2.22	27.65	1.54	$C_9H_{8.7}O_{1.92}S_{0.14}N_{0.018}(OCH_3)_{1.54}$	200.00
L1-Sres		59.31	6.04	0.48	1.73	32.44	0.88	$C_9H_{9.34}O_{3.18}S_{0.11}N_{0.068}(OCH_3)_{0.88}$	199.82
L2-K1		45.53	5.80	0.10	1.10	47.47	0.48	$C_9H_{12.94}O_{6.95}S_{0.03}N_{0.007}(OCH_3)_{0.48}$	248.18
L2-Kres	24.80	46.46	4.75	0.04	1.82	46.90	0.68	$C_9H_{9.74}O_{6.65}S_{0.15}N_{0.008}(OCH_3)_{0.68}$	250.32
L2-S1		47.49	5.19	0.09	0.88	46.35	0.88	$C_9H_{10.24}O_{6.37}S_{0.027}N_{0.006}(OCH_3)_{0.88}$	272.20
L2-Sres	24.73	41.89	4.87	0.02	1.45	27.07[b]	1.47	$C_9H_{10.08}O_{3.6}S_{0.045}N_{0.0014}(OCH_3)_{1.47}$	222.82

[a]Based on C9 units. [b]Determination of the oxygen percentage was done by the difference after ash correction. [c]Oxygen content determined by direct analysis was 38.31% for **L1** and 31.18% for **L2**.

heterogeneity and polydispersity. Furthermore, the line widths would exceed the size of the scalar couplings, causing difficulty in proton spectrum interpretation. Bidimensional experiments are more useful to understand the random nature of the lignin polymer, especially in the correlation of C−H linked in a fused structure. For this purpose, $^1H-^{13}C$ heteronuclear shift correlation spectra of all extracted fractions and the original lignins were acquired to understand the possible changes in linkage density caused by the fractionation procedures. Enlargements in the aliphatic side chain of **L1** and **L2** HSQC spectra are reported in Figure 8, while all lignin fraction spectra and full spectra of **L1** and **L2** are reported in the Supporting Information. In **L2**, the correlation at δ_C 49.0 ppm and δ_H 3.1 ppm is an indication of the presence of $C_\beta-C_{Ar}$ condensation, absent in **L1**. In **L1**, on the other hand, there is a higher presence of $\beta-5$, α-O-4 (cyclic cumarane structures) fusions (δ_C 54.5 ppm, δ_H 3.10). The highly populated signal of OCH_3 (δ_C 56 ppm, δ_H ~3.75 ppm) in **L1** points to the presence of more heterogeneous monomer fusion in this lignin. The correlation Cγ−Hγ of primary alcohols at δ_C 62 ppm and δ_H ~3.35 ppm was observed preferentially in **L1**, while signals related to oxygenated CH_2 (red signal in δ_H 3.6−3.7 ppm and δ_C 56−58 ppm) are observed in **L2**, indicating a more condensed structure. Other differences between the two lignins concern the region of aromatic signals: **L1** showed more populated correlation signals, corresponding to vinyl and aromatic C−H. The correlation signals in **L2** reveal a lower C_{Ar-H} content suggesting further ring condensation. Furthermore, in the **L2** aliphatic C−H spectral range (δ_H 0−2.5 ppm and δ_C 10−40 ppm), no CH_2 signals were detected. This confirms the UV results for **L2** with the greater presence of vinyl units and possible degradation of this lignin.

With Soxhlet fractionation, hot EtOH introduces molecular skeleton modification, recorded as oxygenated CH_2 (δ_H 3.0−4.0 ppm and δ_C 60.0−72.5 ppm) signals in HSQC analysis of **L1-S1** and **L1-S2**. These signals are more populated in **L1-S2**, as a consequence of increased THF solubility conferred by the introduced ether functionalities. This trend is enhanced by the Kumagawa procedure since this apparatus operates at higher temperatures.

Furthermore, **L1-S1** is enriched in vinylic CH_2 (δ_H 6.5−7.0 ppm and δ_C 110.0−120.0 ppm). These signals are not present in the original **L1** lignin, nor in **L1-S2** and **L1-Sres**. These signals appear in all Kumagawa fractions. This suggests the possible occurrence of elimination processes favored by the

https://doi.org/10.1021/acsomega.2c02170
ACS Omega 2022, 7, 25253−25264

temperature treatment, more dramatically occurring during the Kumagawa treatment.

The two fractionation methods yield no significant difference in structural results on **L2**. In both cases, methanol fractions are enriched in oxygenated C−H and display a new signal, compatible with a formate ester (δ_H 8.6−8.5 ppm and δ_C 166.0−168.0 ppm). Interestingly, both **L2-Sres** and **L2-Kres** fractions do not display aromatic C−H correlations: we take this finding as the presence of a large amount of quaternary aryl carbons in **L2** residues and especially as a consequence of the large ash content of **L2**, which is left in the residue by both procedures. This confirms that **L2** underwent a particularly degrading treatment before the solvent fractionation.

Elemental Analyses. Through elemental analyses, we could approximate the molecular formulae for each lignin fraction on the basis of the phenylpropanoid unit (C6-C3), as reported in Table 4. The corresponding formula weights were within the generic range for lignin phenylpropanoid units.[35,36] The compositional values of **L1** and **L2** lignin were corrected by the ash content, detected by combustion of lignin in a muffle furnace at 525 or 600 °C until reaching a constant weight. **L2** lignin displayed a 25.32% total ash content with respect to the much lower value of 3.10% found for **L1** lignin. The ash content of 24.73% found for the **L2** Soxhlet residue (**L2-Sres**) indicates that the extraction leaves most of the ash in the residue, while the **L2** solvent fractions have a negligible ash content. Confirming what was observed from NMR, **L1** fractions presented a molecular formula with a higher OCH_3 content. Elemental analysis revealed a high sulfur content, especially for **L1-S2** (Soxhlet fraction obtained by THF). To the best of our knowledge, precipitation with sulfuric acid is current practice for nonwood lignins, and some of the detected sulfur can be of an inorganic origin rather than an organic counterpart. This residual sulfuric acid can justify the pH measured on **L2** and **L1** lignin suspensions, equal to 9.96 and 6.84, respectively. **L2** lignin, as declared by the provider, was not submitted to acid precipitation but to alkaline treatment, which explains its higher pH. **S1** and **K1** fractions of the two lignins presented a higher nitrogen content and a lower sulfur content than the other respective fractions. In particular, the **L1-S1** fraction displayed the highest nitrogen content: this can be explained considering that ethanol can extract most of the nitrogenous components.[37] Since heating is able to break more labile C-heteroatom bonds, this can explain why the **L1-K1** fraction displays a lower nitrogen content than **L1-S1**. Furthermore, Kumagawa extraction generates the fractions with the lowest sulfur content. Considering that lignin sulfation is often considered to negatively impact lignin processability and application perspectives, this aspect is expected to make the Kumagawa extraction fractions preferable to Soxhlet fractions.

All fractions isolated from the Kumagawa or Soxhlet treatment were richer in oxygen than the original lignin. This was expected for **L1** fractions, which, according to HSQC, were enriched in oxygen by ethanol binding. Therefore, we hypothesize that alcohol functionalization took place during the alcohol treatment, and the relative products were extracted by alcoholic solvents and THF, while most oxidized and compromised fractions were left in the residues.

CONCLUSIONS

The focus of this work was to determine the impact of solvent extraction processes and solvent nature on lignin fractions to enable lignin with controlled properties. We compared the results of two fractionation methods, the Soxhlet and Kumagawa extraction with hot solvents. We selected two commercial technical lignins and our analysis revealed that they presented quite different properties: while **L1** lignin was rich in carbonyl groups and stilbene units, **L2** presented a more depolymerized structure and abundant phenyl ether moieties. GPC analyses of the acetylated fractions showed a decrease in the molecular weight and a narrower molecular weight distribution yielded by the fractionation. The chemical characterization of extracted fractions revealed that the chemical composition of the soluble fractions is dependent upon the nature of the extraction solvent, while the extraction yield depends on the fractionation process. Indeed, the fractionation of the two lignins revealed the capacity of the Kumagawa process to increase extraction yields, especially for **L1**. Furthermore, THF used as a solvent in the Kumagawa process produced fractions with a higher ratio of carbonyl over other oxidized moieties. The Kumagawa extraction is particularly effective on lignin, which was not previously submitted to degrading processes and is rich in carbonyl groups. In the case of **L1**, the Kumagawa treatment allows one to maximize the extraction yield leaving a minimal residue (25 vs 67% in Soxhlet fractionation), thus achieving high extraction yields. This happens because hot ethanol treatment modifies lignin's molecular skeleton, enhancing its THF solubility. Conversely, an extensively depolymerized lignin, such as **L2**, only shows a slight increase in the fractionation yield by Kumagawa extraction. This lignin is so much degraded that alcohol treatment does not appreciably modify its solubility. Furthermore, the Kumagawa process presents a higher tendency of heteroatoms' (N, S) cleavage due to a higher temperature of the extraction thimble. Our study gives important insights into structure−property relationships based on the solvent solubility in view of their potential further utilization for the development of biobased chemicals.

ASSOCIATED CONTENT

Supporting Information

The Supporting Information is available free of charge at https://pubs.acs.org/doi/10.1021/acsomega.2c02170.

Pyrolysis products determined by Py-GC/MS, ^{13}C NMR spectra and HSQC experiments of all lignin samples, and full window ATR-FTIR spectra of all lignin samples (PDF)

AUTHOR INFORMATION

Corresponding Author

Alessandra Operamolla − *Dipartimento di Chimica e Chimica Industriale, Università di Pisa, I-56124 Pisa, Italy; Interuniversity Consortium of Chemical Reactivity and Catalysis (CIRCC), I-70126 Bari, Italy;* orcid.org/0000-0001-8527-0920; Email: alessandra.operamolla@unipi.it

Authors

Rosarita D'Orsi − *Dipartimento di Chimica e Chimica Industriale, Università di Pisa, I-56124 Pisa, Italy; Interuniversity Consortium of Chemical Reactivity and Catalysis (CIRCC), I-70126 Bari, Italy*

https://doi.org/10.1021/acsomega.2c02170
ACS Omega 2022, 7, 25253−25264

Jeannette J. Lucejko − *Dipartimento di Chimica e Chimica Industriale, Università di Pisa, I-56124 Pisa, Italy; Center for Instrument Sharing of the University of Pisa (CISUP), University of Pisa, I-56126 Pisa, Italy*

Francesco Babudri − *Dipartimento di Chimica, Università degli Studi di Bari Aldo Moro, I-70126 Bari, Italy;* orcid.org/0000-0002-0227-8087

Complete contact information is available at: https://pubs.acs.org/10.1021/acsomega.2c02170

Author Contributions

This manuscript was written through contributions of all authors. All authors have given approval to the final version of the manuscript.

Funding

This research received financial support from the University of Pisa through the project "BIHO 2021-Bando Incentivi di Ateneo Horizon e Oltre" (D.d. 408, Prot. No. 0030596/2021) and through the project PRA_2020_21 "SUNRISE: Concentratori solari luminescenti NIR riflettenti".

Notes

The authors declare no competing financial interest.

■ ACKNOWLEDGMENTS

Dr. Lorella Marchetti and Dr. Mario Cifelli are acknowledged for instructing R.D. to use JEOL Delta software. Dr. Antonella Manariti and Dr. Pietro Cotugno are acknowledged for fruitful scientific discussions. The authors thank the Center for Instrument Sharing of the University of Pisa (CISUP) for the access to the ATR-FTIR facility and for providing Py-GC−MS measurements.

■ ABBREVIATIONS

L1, kraft lignin with acid post-treatment; **L2**, kraft lignin with alkaline post-treatment; THF, tetrahydrofuran; DMSO, dimethyl sulfoxide; ATR-FTIR, attenuated total reflection-Fourier transform infrared spectroscopy; GPC, gel permeation chromatography; NMR, nuclear magnetic resonance; HSQC, heteronuclear single quantum coherence; GC, gas chromatography; MS, mass spectrometry; Py, Pyrolysis

■ REFERENCES

(1) Lignin, Biosynthesis and Transformation for Industrial Applications. In *Springer Series on Polymer and Composite Materials*, Sharma, S.; Kumar, A., Eds.; Springer Nature: Switzerland AG, 2020.

(2) Ragauskas, A. J.; Beckham, G. T.; Biddy, M. J.; Chandra, R.; Chen, F.; Davis, M. F.; Davison, B. H.; Dixon, R. A.; Gilna, P.; Keller, M.; Langan, P.; Naskar, A. K.; Saddler, J. N.; Tschaplinski, T. J.; Tuskan, G. A.; Wyman, C. E. Lignin Valorization: Improving Lignin Processing in the Biorefinery. *Science* **2014**, *344*, No. 1246843.

(3) Bajwa, D. S.; Pourhashem, G.; Ullah, A. H.; Bajwa, S. G. A concise review of current lignin production, applications, products and their environmental impact. *Ind. Crops Prod.* **2019**, *139*, No. 111526.

(4) Parsell, T.; Yohe, S.; Degenstein, J.; Jarrell, T.; Klein, I.; Gencer, E.; Hewetson, B.; Hurt, M.; Kim, J. I.; Choudhari, H.; Saha, B.; Meilan, R.; Mosier, N.; Ribeiro, F.; Delgass, W. N.; Chapple, C.; Kenttämaa, H. I.; Agrawal, R.; Abu-Omar, M. M. A Synergistic Biorefinery Based on Catalytic Conversion of Lignin Prior to Cellulose Starting from Lignocellulosic Biomass. *Green Chem.* **2015**, *17*, 1492−1499.

(5) Aro, T.; Fatehi, P. Production and Application of Lignosulfonates and Sulfonated Lignin. *ChemSusChem* **2017**, *10*, 1861−1877.

(6) Isikgor, F. H.; Becer, C. R. Lignocellulosic biomass: a sustainable platform for the production of bio-based chemicals and polymers. *Polym. Chem.* **2015**, *6*, 4497−4559.

(7) Allegretti, C.; Fontanay, S.; Krauke, Y.; Luebbert, M.; Strini, A.; Troquet, J.; Turri, S.; Griffini, G.; D'Arrigo, P. Two-Step Fractionation of a Model Technical Lignin by Combined Organic Solvent Extraction and Membrane Ultrafiltration. *ACS Sustainable Chem. Eng.* **2018**, *6*, 9056−9064.

(8) Pandey, M. P.; Kim, C. S. Lignin Depolymerization and Conversion: A Review of Thermochemical Methods. *Chem. Eng. Technol.* **2011**, *34*, 29−41.

(9) Zhao, C.; Xie, S.; Pu, Y.; Zhang, R.; Huang, F.; Ragauskas, A. J.; Yuan, J. S. Synergistic Enzymatic and Microbial Lignin Conversion. *Green Chem.* **2016**, *18*, 1306−1312.

(10) Alriols, M. G.; García, A.; Llano-Ponte, R.; Labidi, J. Combined organosolv and ultrafiltration lignocellulosic biorefinery process. *Chem. Eng. J.* **2010**, *157*, 113−120.

(11) Stone, M. L.; Anderson, E. M.; Meek, K. M.; Reed, M.; Katahira, R.; Chen, F.; Dixon, R. A.; Beckham, G. T.; Roman-Leshkov, Y. Reductive Catalytic Fractionation of C-Lignin. *ACS Sustainable Chem. Eng.* **2018**, *6*, 11211−11218.

(12) Anderson, E. M.; Stone, M. L.; Hülsey, M. J.; Beckham, G. T.; Roman-Leshkov, Y. Kinetic Studies of Lignin Solvolysis and Reduction by Reductive Catalytic Fractionation Decoupled in Flow-Through Reactors. *ACS Sustainable Chem. Eng.* **2018**, *6*, 7951−7959.

(13) Gosselink, R. J. A.; de Jong, E.; Guran, B.; Abächerli, A. Co-ordination network for lignin: standardisation, production and applications adapted to market requirements. *Ind. Crops Prod.* **2004**, *20*, 121−129.

(14) Fernández-Rodríguez, J.; Erdocia, X.; Hernández-Ramos, F.; Alriols, M. G.; Labidi, J. Lignin Separation and Fractionation by Ultrafiltration. In *Separation of Functional Molecules in Food by Membrane Technology*,Charis, M., Ed.; Academic Press, 2019; pp 229−265.

(15) Biermann, C. J. *Handbook of Pulping and Papermaking*, 2nd ed.; Academic Press: San Diego, California, 1996.

(16) Berton, P.; Manouchehr, S.; Wong, K.; Ahmadi, Z.; Abdelfatah, E.; Robin, D.; Rogers, R. D.; Bryant, S. L. Ionic Liquids-Based Bitumen Extraction: Enabling Recovery with Environmental Footprint Comparable to Conventional Oil. *ACS Sustainable Chem. Eng.* **2020**, *8*, 632−641.

(17) Thielemans, W.; Woll, R. P. Lignin esters for use in unsaturated thermosets: lignin modification and solubility modeling. *Biomacromolecules* **2005**, *6*, 1895−1905.

(18) Cateto, C. A.; Barreiro, M. F.; Rodrigues, A. E.; Brochier-Salon, M. C.; Thielemans, W.; Belgacem, M. N. Lignins as macromonomers for polyurethane synthesis: a comparative study on hydroxyl groups determination. *J. Appl. Polym. Sci.* **2008**, *109*, 3008−3017.

(19) Galletti, G. C.; Bocchini, P. Pyrolysis/gas chromatography/mass spectrometry of lignocellulose. *Rapid Commun. Mass Spectrom.* **1995**, *9*, 815−826.

(20) Ralph, J.; Hatfield, R. D. Pyrolysis-GC-MS characterization of forage materials. *J. Agric. Food Chem.* **1991**, *39*, 1426−1437.

(21) Tobias, K. http://www.amdis.net/.

(22) Passoni, V.; Scarica, C.; Levi, M.; Turri, S.; Griffini, G. Fractionation of Industrial Softwood Kraft Lignin: Solvent Selection as a Tool for Tailored Material Properties. *ACS Sustainable Chem. Eng.* **2016**, *4*, 2232−2242.

(23) Domínguez-Robles, J.; Tamminen, T.; Liitia, T.; Peresin, M. S.; Rodríguez, A.; Jääskeläinen, A.-S. Aqueous acetone fractionation of kraft, organosolv and soda lignins. *Int. J. Biol. Macromol.* **2018**, *106*, 979−987.

(24) Cheng, C.; Truong, J.; Barrett, J. A.; Shen, D.; Abu-Omar, M. M.; Ford, P. C. Hydrogenolysis of organosolv lignin in ethanol/isopropanol media without added transition metal catalyst. *ACS Sustainable Chem. Eng.* **2020**, *8*, 1023−1030.

(25) Agarwal, U. P.; Atalla, R. H. Vibrational Spectroscopy. In*Lignin and Lignans*, Heitner, C.; Dimmel, D. R.; Schmidt, J. A., Eds.; CrC Press: Boca Raton, 2010.

(26) Faix, O. Fourier Transform Infrared Spectroscopy. In*Methods in Lignin Chemistry*,Lin, S. Y.; Dence, C. W., Eds.; Springer-Verlag: Heidelberg, Germany, 1992; pp 233−241.
(27) Wang, K.; Xu, F.; Sun, R. Molecular Characteristics of Kraft-AQ Pulping Lignin Fractionated by Sequential Organic Solvent Extraction. *Int. J. Mol. Sci.* **2010**, *11*, 2988−3001.
(28) Yuan, T.-Q.; He, J.; Xu, F.; Sun, R.-C. Fractionation and physico-chemical analysis of degraded lignins from the black liquor of Eucalyptus pellita KP-AQ pulping. *Polym. Degrad. Stab.* **2009**, *94*, 1142−1150.
(29) Gärtner, A.; Gellerstedt, G.; Tamminen, T. Determination of phenolic hydroxyl groups in residual lignin using a modified UV-method. *Nord. Pulp Pap. Res. J.* **1999**, *14*, 163−170.
(30) Yamasaki, T.; Hosoya, S.; Chen, C-L.; Gtratzl, J.; Chang, H.-M. Characterization of residual lignin in kraft pulp. *Int. Symp. Wood Pulping Chem.* **1981**, *2*, 34−42.
(31) Gellerstedt, G.; Lindfors, E.-L. On the formation of enol ether structures in lignin during kraft cooking. *Nord. Pulp Pap. Res. J.* **1987**, *2*, 71−75.
(32) Dence, C. W.; Lin, S. Y., Eds.;*Methods in Lignin Chemistry*; Springer-Verlag: Heidelberg, 1992.
(33) Zakis, G. F. *Functional Analysis of Lignins and Their Derivatives*; Tappi Press: Atlanta, 1994.
(34) Alekhina, M.; Ershova, O.; Ebert, A.; Heikkinen, S.; Sixta, H. Softwood kraft lignin for value-added applications: Fractionation and structural characterization. *Ind. Crops Prod.* **2015**, *66*, 220−228.
(35) Chen, L. C. Lignin and Lignan Biosynthesis. In*ACS Symposium Series*, Lewis, N. G.; Sarkanen, S., Eds.; American Chemical Society: Washington, DC, 1998; p 255.
(36) El Mansouri, N.-E.; Salvadó, E. Structural Characterization of Technical Lignins for the Production of Adhesives: Application to Lignosulfonate, Kraft, Soda-Anthraquinone, Organosolv and Ethanol Process Lignins. *Ind. Crops Prod.* **2006**, *24*, 8−16.
(37) Sánchez, R. J.; Fernández, M. B.; Nolasco, S. M. Ethanol extraction of canola oil: Kinetics and effects of type of solvent and microwave-pretreatment. *OCL* **2019**, *26*, No. 27.

https://doi.org/10.1021/acsomega.2c02170
ACS Omega 2022, 7, 25253−25264